

Identify the topological superconducting order in a multi-band quantum wire

Pei Wang*,^{1,2,*} Jie Liu*,³ Qing-feng Sun,^{1,4} and X. C. Xie^{1,4}

¹International Center for Quantum Materials, School of Physics, Peking University, Beijing 100871, China

²Institute of Applied Physics, Zhejiang University of Technology, Hangzhou 310023, China

³Applied Physics Department, Xi'an Jiaotong University, Xi'an 710049, China

⁴Collaborative Innovation Center of Quantum Matter, Beijing 100871, China

(Dated: October 16, 2014)

How to distinguish the zero-bias peak (ZBP) caused by the Majorana fermions from that by the other effects remains a challenge in detecting the topological order of a quantum wire. In this paper we propose to distinguish the topological superconducting phase from the topologically trivial phase by making a Josephson junction of the quantum wire attached to a side lead and then measuring the tunneling conductance through it as the phase difference across the junction ϕ varies. Even if the ZBPs exist in both phases, we can identify the topological superconducting phase by a conductance peak at $\phi = \pi$ and a nearby butterfly pattern.

Introduction.— Recently the topological superconductor (TSC) has been a focus of attention because it hosts the Majorana fermions which have potential applications in the topological quantum computation. Among various proposals of realizing the TSC, a quantum wire with strong spin-orbit coupling and proximity-induced superconductivity^{1–4} attracts particular interests due to its easily being implemented. While the nanowires of InSb and InAs^{5–8} have been manufactured as the candidates of TSCs, the detection of topological order and Majorana fermions keeps a highly nontrivial problem.

A TSC quantum wire has the Majorana fermions as its edge excitations. The Majorana fermion leads to a zero-bias peak (ZBP) in the tunneling conductance^{9–13}, which was recently observed in experiments^{5–8}. However, the ZBP by itself cannot exclusively sign a topologically nontrivial Majorana fermion, since the disorder in quantum wires may induce the sub-gap Andreev levels close to zero energy, which cause similar ZBPs in the topologically trivial phase^{14,15}. Furthermore, the observed ZBP may also be caused by the Kondo effect¹⁶, 0.7 anomaly⁸ or weak antilocalization¹⁷. Only the Majorana fermions in the TSC phase can be used for the quantum computation^{18–21}, it is then obliged to study how to distinguish the topologically trivial and nontrivial phases in the quantum wire. Some authors invoked the non-local properties of Majorana fermions exhibited in the current-current correlations^{22–24} or the dependence of the ZBP on the confining potential at the opposite end of the wire²⁵. The others kept on exploiting the local properties of Majorana fermions in the selective equal-spin Andreev reflections²⁶, the conductance of a quantum dot that is coupled to a TSC²⁷, the scaling property of the conductance at finite temperatures with a resistive lead²⁸, or the tunneling process with the ferromagnetic leads²⁹. Whereas these suggestions either require a measurement of the correlations which is difficult to implement or do not systematically consider the effect of the casual Andreev bound level whose local properties are similar to those of a Majorana fermion.

In this paper, we propose to distinguish the topologically trivial and nontrivial phases in a quantum wire by

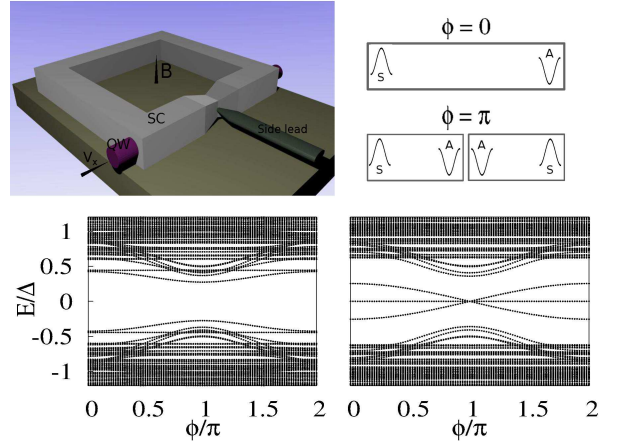


FIG. 1. [Color online]. [Left top panel] The schematic diagram of our proposal. A quantum wire (QW) is covered by the ring-shaped superconducting layer (SC) which forms a Josephson junction at the middle of the wire. A side lead is connected to the junction to measure the tunneling conductance. A parallel magnetic field V_x is necessary for generating the topological order. While a transverse field B is applied to tune the phase difference ϕ across the junction. [Right top panel] There are a symmetric Majorana fermion (S) and an antisymmetric one (A) at the ends of the wire, respectively, if the superconducting phase is uniform throughout the wire. But if a π -phase difference is across the junction, two additional Majorana fermions with the same symmetry will emerge at the junction. [Bottom panels] The eigenenergy spectra of \hat{H}_w in the TSC phase at $\mu = -2t$ (right bottom panel) and in the trivial phase at $\mu = -2t + 4\Delta$ (left bottom panel).

coupling a side lead (or a STM tip) to its center where the proximity-induced superconductivity is weakened to a weak coupling, i.e., a Josephson junction. Fig. 1 (left top panel) shows the schematic diagram of our proposal. It was known^{3,30–33} that in the TSC phase a pair of Majorana fermions emerge at the center of the Josephson junction with the coupling energy proportional to $\cos(\phi/2)$ where ϕ is the phase difference across the junction. These Majorana fermions induce the well-known

fractional Josephson effect (FJE). Several experiments were conducted for observing the putative 4π -periodic FJE^{34,35}, but failed due to the parity-flipping processes. It is surprising that we can distinguish these Majorana fermions from the trivial zero-energy Andreev bound states with the help of a side lead, because the Majorana fermions have the same symmetry in their particle-hole wave functions (Fig. 1, right top panel) which leads to a constructive interference in the tunneling process. Even if the ZBP exists in both the TSC and the trivial phases, it splits into three peaks in the TSC phase as ϕ deviates from π , displaying a butterfly pattern, but keeps invariant in the trivial phase. A conductance peak at $\phi = \pi$ and a nearby butterfly pattern are the fingerprints of the TSC phase.

The key difference between our proposal and previous ones is the utilization of an additional degree of freedom, i.e., the phase difference ϕ , which can be tuned by applying a transverse magnetic field \mathbf{B} . This magnetic field is screened by the superconducting layer and does not affect the quantum wire directly. The effects disguising themselves as Majorana fermions, e.g., the disorder effect, the Kondo effect, etc., are indifferent to the superconducting phase, so that they can be ruled out by the conductance peak at $\phi = \pi$. Finally, our proposal only requires measuring the tunneling conductance through the side-lead and is practicable in current techniques.

Theoretical model of the quantum wire.— We simulate the quantum wire in the x direction by a rectangular lattice of size $(N_x \times N_y)$ lying in the $x-y$ plane with the Hamiltonian:

$$\begin{aligned} \hat{H}_w = & \sum_{\vec{R}, \vec{d}, \alpha} -t(\vec{R}, \vec{d}) \hat{\psi}_{\vec{R}+\vec{d}, \alpha}^\dagger \hat{\psi}_{\vec{R}, \alpha} - \mu \sum_{\vec{R}, \alpha} \hat{\psi}_{\vec{R}, \alpha}^\dagger \hat{\psi}_{\vec{R}, \alpha} \\ & - iU_R \sum_{\vec{R}, \vec{d}, \alpha, \beta} \hat{\psi}_{\vec{R}+\vec{d}, \alpha}^\dagger \left(\vec{z} \cdot (\vec{\sigma}_{\alpha\beta} \times \vec{d}) \right) \hat{\psi}_{\vec{R}, \beta} \\ & + V_x \sum_{\vec{R}, \alpha, \beta} \hat{\psi}_{\vec{R}, \alpha}^\dagger (\sigma_x)_{\alpha\beta} \hat{\psi}_{\vec{R}, \beta} \\ & + \sum_{\vec{R}, \alpha} \left(\Delta(\vec{R}) \hat{\psi}_{\vec{R}, \alpha}^\dagger \hat{\psi}_{\vec{R}, -\alpha}^\dagger + h.c. \right), \end{aligned} \quad (1)$$

where \vec{R} denotes the lattice sites, \vec{d} the unit vectors connecting the nearest neighbor sites in the x and y directions, α and β the spins, μ the chemical potential, U_R the Rashba coupling, \vec{z} the unit vector along the z direction, and $\vec{\sigma}$ the Pauli matrices. V_x is a magnetic field along the wire for generating the topological order. The on-site superconducting pairing $\Delta(\vec{R})$ equals to Δ and $\Delta e^{i\phi}$ in the left and right sides of the Josephson junction respectively, with ϕ denoting the phase difference across the junction which is tuned by a transverse magnetic field. Finally, a barrier arises from the weakened superconductivity at the junction, which is simulated by a suppressed nearest-neighbor hopping, i.e., we set $t(\vec{R}, \vec{d}) = t$ for most (\vec{R}, \vec{d}) but $t(\vec{R}, \vec{d}) = t' < t$ if \vec{R} and $(\vec{R} + \vec{d})$ locate at different sides of the junction.

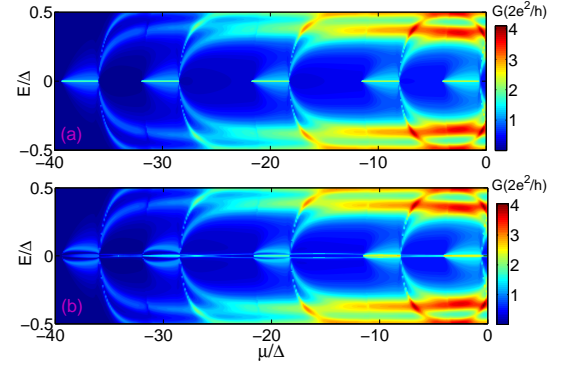


FIG. 2. [Color online] The 3D plot of the conductance G as a function of the chemical potential μ and the voltage bias E at (a) $\lambda = 0, \epsilon = 0.001t$ and (b) $\lambda = 0.3, \epsilon = 0.001t$. The unit of G is $2e^2/h$.

We emphasize that the weak coupling ($t' < t$) is a necessary condition for distinguishing the TSC phase from the trivial phase by inducing an avoided crossing in the spectrum of the latter. We choose the parameters in the tight-binding model that match the corresponding values in recent experiments¹⁴: $\Delta = 250\mu\text{eV}$, $t = 10\Delta$, $V_x = 2\Delta$ and $U_R = 2\Delta$, and set the coupling at the junction to $t' = 0.5t$. The dimensions of the wire are $N_x a = 200a \approx 4\mu\text{m}$ and $N_y a = 5a \approx 100\text{nm}$.

The quasi-one-dimensional wire has 10 transverse subbands. It is a TSC so long as an odd number of subbands are occupied^{36,37}. By varying the chemical potential μ , we observe a sequence of TSC phases well separated by the topologically trivial phases. In the TSC phase, a pair of Majorana bound states are located at the ends of the wire regardless of the value of ϕ (Fig. 1, right bottom panel). At the same time, an additional pair of sub-gap Andreev levels cross each other at $\phi = \pi$, corresponding to two Majorana bound states located at the junction. They have the same symmetry in their particle-hole wave functions, so that the coupling between them vanishes at $\phi = \pi$. In the topologically trivial phase, however, the sub-gap levels do not cross, but avoid each other instead, so that there is no Majorana bound states (Fig. 1, left bottom panel).

Topologically trivial sub-gap Andreev levels.— The disorder in a quantum wire may casually generate a pair of Andreev bound levels near zero energy in the topologically trivial phase, which cause a ZBP in the tunneling spectroscopy just like the Majorana fermions^{14,15}. For simulating these topologically trivial sub-gap Andreev levels, we introduce an additional localized impurity state

$$\hat{H}_d = \epsilon \hat{d}^\dagger \hat{d} + \lambda (\hat{d}^\dagger \hat{\psi}_{\vec{R}_J, \alpha} + h.c.), \quad (2)$$

where \hat{d} denotes the field operator of the impurity state located at \vec{R}_J near the junction, which is weakly coupled to the wire (λ is small). And we set a sufficiently small ϵ so that the Andreev levels are close to zero energy.

Tunneling spectroscopy at the junction.— We use the local tunneling spectroscopy at the Josephson junction to distinguish the topological superconducting phase from the trivial phase. We attach a side lead (or a STM tip), which has a fixed density of states at the Fermi energy, close to the junction. The differential conductance in the side lead at a voltage bias E is expressed as^{14,38,39}

$$G(E) = \Gamma_{Le} G_{eh}^r(E) \Gamma_{Lh} G_{eh}^a(E), \quad (3)$$

where $\Gamma_{Le} = \Gamma_{Lh} = 0.1t$ are the line-widths of the side lead with the electron's part and the hole's part, respectively. $G_{eh}^{r(a)}$ is the retarded (advanced) Green's function of the system (see more details of the calculation in Ref. 14). We set the temperature to zero in Eq. (3). But our conclusions keep valid at finite temperatures.

Changing the chemical potential μ tunes the topological order of the system. We first study the conductance function $G(E)$ at different chemical potentials, while fixing the phase difference across the junction to $\phi = \pi$ (see Fig. 2). In the absence of the impurity Andreev levels ($\lambda = 0$ in Eq. (2)), there are a unique pair of Majorana states located at the junction in the TSC phase, but no in the trivial phase. This pair of Majorana fermions have the same symmetry, which leads to a constructive interference in the tunneling process. Since $G(E)$ reflects the local density of states at the junction, a ZBP emerges in $G(E)$ in the TSC phase, but is absent in the trivial phase. In Fig. 2(a), we clearly see a group of bright narrow lines at $E = 0$ which distinguish the TSC regions from the trivial regions. There are totally five TSC regions, corresponding to 1, 3, 5, 7 and 9 occupied subbands respectively.

Unfortunately, a pair of impurity Andreev levels close to zero energy will cause a similar ZBP in whatever the TSC or the trivial phases. This is shown in Fig. 2(b), where we choose the small but non-zero λ and ϵ . Compared with Fig. 2(a), a bright line at $E \approx 0$ is now through the whole region of μ , so that one cannot distinguish the TSC and the trivial phases any more. With the model ($\hat{H}_w + \hat{H}_d$) we successfully reproduce the results in Refs. 14 and 15, i.e., a ZBP by itself cannot identify the topological superconducting phase and the nontrivial Majorana fermions.

We propose to distinguish the TSC phase from the trivial phase by the behavior of the conductance as the superconducting phase difference ϕ varies. In the TSC phase, at $\phi = \pi$ the two adjacent Majorana bound states at the junction contribute to a conductance of $4e^2/h$. As ϕ deviates from π , the two Majorana modes are coupled and push each other away from zero energy, so that the zero-bias conductance quickly decreases and the ZBP is split into two side peaks at finite biases. This evolution is displayed in Fig. 3(b), where the conductance function $G(E, \phi)$ shows a butterfly pattern centered at $E = 0$ and $\phi = \pi$. In the topologically trivial phase (Fig. 3(a)), however, there is no ZBP whatever ϕ is. As ϕ varies, the sub-gap Andreev levels avoid each other, so that the zero-bias conductance is always absent, indifferent to ϕ . Whereas

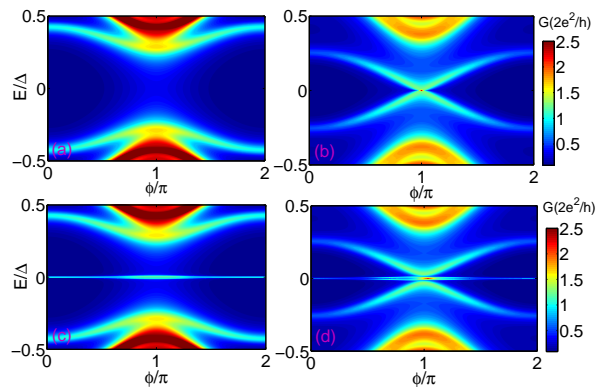


FIG. 3. [Color online] The evolution of the conductance as ϕ varies at four different points of Fig. 2. (a) $\mu = -2t + 4\Delta$ and $\lambda = 0, \epsilon = 0.001t$. (b) $\mu = -2t$ and $\lambda = 0, \epsilon = 0.001t$. (c) $\mu = -2t + 4\Delta$ and $\lambda = 0.3, \epsilon = 0.001t$. (d) $\mu = -2t$ and $\lambda = 0.3, \epsilon = 0.001t$.

the presence of impurities, disorder effect, Kondo effect, etc., may induce a ZBP in the trivial phase, causing that one can not distinguish the TSC phase from the trivial phase by the ZBP alone¹⁴. However, this casual ZBP keeps invariant as ϕ varies, and no butterfly pattern is observed (Fig. 3(c)). The difference between the TSC and the trivial phases is clearly reflected in the tunneling spectroscopy. Therefore, by utilizing an additional degree of freedom ϕ , we can distinguish the topologically trivial and nontrivial phases according to whether the ZBP at $\phi = \pi$ splits while ϕ deviates from π .

Furthermore, this criterion keeps valid in the coexistence of the casual ZBP caused by the disorder effect and the ZBP by the Majorana modes. In this dirty TSC phase, the zero-bias conductance $G(E = 0)$ shows a peak at $\phi = \pi$ due to the nontrivial Majorana fermions over the background signal contributed by the impurity levels. As ϕ deviates from π , the unique ZBP is split into three peaks: two peaks are symmetric to zero, resulting in a butterfly pattern, and the third one keeps at $E = 0$ (Fig. 3(d)). This behavior is significantly different from that in the topologically trivial phase as shown in Fig. 3(a) and (c). In summary, with the help of the superconducting phase difference ϕ , we can distinguish all the four cases: the trivial phase without the casual ZBP, the TSC phase without the casual ZBP, the trivial phase with the casual ZBP, and the TSC phase with the casual ZBP. Here a butterfly pattern in the conductance function $G(E, \phi)$ is the key characteristic of the TSC phase.

The Majorana fermions at the junction are localized in a small area of the wire, so that the side lead may not be precisely coupled to them in experiments. We demonstrate that our conclusions are not sensitive to the position where the side lead is coupled. In Fig. 4, we display the conductance $G(E, \phi)$ as the side lead gradually moves away from the junction, whereas the impurity levels are present and fixed at the junction. The fingerprint of the TSC phase, i.e., the butterfly pattern, can be clearly ob-

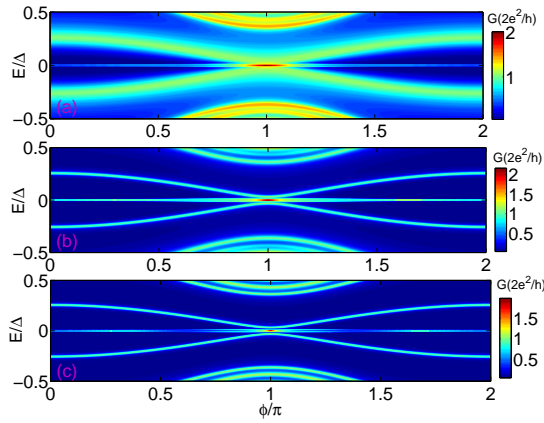


FIG. 4. [Color online] The 3D plot of the conductance function $G(E, \phi)$ when the side lead is coupled to different positions of the quantum wire. From top to bottom, the distance between the side lead and the Josephson junction is (a) 1 site, (b) 5 sites and (c) 10 sites, respectively. The other parameters keep the same as in Fig. 3(d).

served even if the side lead has been 10 sites far away from the junction (corresponding to $200nm$ with our parameters). As the side lead moves away, its coupling with the Majorana fermions becomes weaker, so that the conduc-

tance peak becomes narrower ($\Delta\phi$ decreases). But the height of the peak always keeps invariant at zero temperature. Whereas at finite temperatures, the conductance peak will be suppressed when the side lead leaves the junction. But the butterfly pattern is still distinguishable, as long as the temperatures $k_B T$ is no greater than the ZBP splitting, i.e., about 0.2Δ in Fig. 4.

Conclusions.— We conclude that the topological superconducting phase in a quantum wire can be distinguished from the trivial phase by the behavior of the side-lead conductance as the phase difference across the Josephson junction varies. The TSC phase is identified by a conductance peak in $G(\phi)$ at $\phi = \pi$. A more elaborate criterion is a butterfly pattern in the function $G(E, \phi)$, i.e., the splitting of the zero bias peak as ϕ deviates from π . In the topologically trivial phase, however, there is either no zero-bias peak or a casual zero-bias peak that keeps invariant as ϕ varies. This offers an exclusive sign for the topological superconducting phase.

Acknowledgement.— This work is supported by NSFC (Grants Nos. 11304280, 91221302 and 11274364), NBRP of China (Grants Nos. 2012CB821402, 2012CB921303 and SQ2015CB090460) and CPSF (Grant No. 2014M550542).

* P. Wang and J. Liu contributed equally to this work.

* wangpei@zjut.edu.cn

- ¹ J. D. Sau, R. M. Lutchyn, S. Tewari, and S. Das Sarma, Phys. Rev. Lett. **104**, 040502 (2010).
- ² J. Alicea, Phys. Rev. B **81**, 125318 (2010).
- ³ R. M. Lutchyn, J. D. Sau, and S. Das Sarma, Phys. Rev. Lett. **105**, 077001 (2010).
- ⁴ Y. Oreg, G. Refael, and F. von Oppen, Phys. Rev. Lett. **105**, 177002 (2010).
- ⁵ V. Mourik, K. Zuo, S. M. Frolov, S. R. Plissard, E. P. A. M. Bakkers, and L. P. Kouwenhoven, Science **336**, 1003 (2012).
- ⁶ M. T. Deng, C. L. Yu, G. Y. Huang, M. Larsson, P. Caroff, and H. Q. Xu, Nano Lett. **12**, 6414 (2012).
- ⁷ A. Das, Y. Ronen, Y. Most, Y. Oreg, M. Heiblum, and H. Shtrikman, Nature Physics **8**, 887 (2012).
- ⁸ H. O. H. Churchill, V. Fatemi, K. Grove-Rasmussen, M. T. Deng, P. Caroff, H. Q. Xu, and C. M. Marcus, Phys. Rev. B **87**, 241401(R) (2013).
- ⁹ K. T. Law, P. A. Lee, and T. K. Ng, Phys. Rev. Lett. **103**, 237001 (2009).
- ¹⁰ K. Flensberg, Phys. Rev. B **82**, 180516(R) (2010).
- ¹¹ J. D. Sau, S. Tewari, R. M. Lutchyn, T. D. Stanescu, and S. Das Sarma, Phys. Rev. B **82**, 214509 (2010).
- ¹² M. Wimmer, A. R. Akhmerov, J. P. Dahlhaus, and C. W. J. Beenakker, New Journal of Physics **13**, 053016 (2011).
- ¹³ A. R. Akhmerov, J. P. Dahlhaus, F. Hassler, M. Wimmer, and C. W. J. Beenakker, Phys. Rev. Lett. **106**, 057001 (2011).
- ¹⁴ J. Liu, A. C. Potter, K. T. Law, and P. A. Lee, Phys. Rev. Lett. **109**, 267002 (2012).
- ¹⁵ D. Bagrets and A. Altland, Phys. Rev. Lett. **109**, 227005 (2012).
- ¹⁶ E. J. H. Lee, X. Jiang, R. Aguado, G. Katsaros, C. M. Lieber, and S. De Franceschi, Phys. Rev. Lett. **109**, 186802 (2012).
- ¹⁷ D. I. Pikulin, J. P. Dahlhaus, M. Wimmer, H. Schomerus, C. W. J. Beenakker, New J. Phys. **14**, 125011 (2012).
- ¹⁸ J. Alicea, Y. Oreg, G. Refael, F. von Oppen, and M. P. A. Fisher, Nature Phys. **7**, 412 (2011).
- ¹⁹ A. Romito, J. Alicea, G. Refael, and F. von Oppen, Phys. Rev. B **85**, 020502(R) (2012).
- ²⁰ J. D. Sau, D. J. Clarke, and S. Tewari, Phys. Rev. B **84**, 094505 (2011).
- ²¹ B. van Heck, A. R. Akhmerov, F. Hassler, M. Burrello, and C. W. J. Beenakker, New J. Phys. **14**, 035019 (2012).
- ²² C. J. Bolech and E. Demler, Phys. Rev. Lett. **98**, 237002 (2007).
- ²³ S. Bose and P. Sodano, New Journal of Physics **13**, 085002 (2011).
- ²⁴ J. Liu, F.-C. Zhang, and K. T. Law, Phys. Rev. B **88**, 064509 (2013).
- ²⁵ T. D. Stanescu and S. Tewari, Phys. Rev. B **89**, 220507(R) (2014).
- ²⁶ J. J. He, T. K. Ng, P. A. Lee, and K. T. Law, Phys. Rev. Lett. **112**, 037001 (2014).
- ²⁷ D. E. Liu and H. U. Baranger, Phys. Rev. B **84**, 201308(R) (2011).
- ²⁸ D. E. Liu, Phys. Rev. Lett. **111**, 207003 (2013).
- ²⁹ C. D. Ren, K. S. Chan, and J. Wang, J. Phys.: Condens. Matter **26**, 175702 (2014).
- ³⁰ A. Y. Kitaev, Phys. Usp. **44** (suppl.), 131 (2001).
- ³¹ H.-J. Kwon, K. Sengupta, and V. M. Yakovenko, Eur.

- Phys. J. B **37**, 349 (2004).
- ³² L. Fu and C. L. Kane, Phys. Rev. B **79**, 161408(R) (2009).
- ³³ L. Jiang, D. Pekker, J. Alicea, G. Refael, Y. Oreg, and F. von Oppen, Phys. Rev. Lett. **107**, 236401 (2011).
- ³⁴ S. Hart, H. Ren, T. Wagner, P. Leubner, M. Mühlbauer, C. Brüne, H. Buhmann, L. W. Molenkamp, and A. Yacoby, Nat. Phys. **10**, 638 (2014).
- ³⁵ V. S. Pribiag, A. J. A. Beukman, F. Qu, M. C. Cassidy, C. Charpentier, W. Wegscheider, and L. P. Kouwenhoven, arXiv:1408.1701 [cond-mat.mes-hall].
- ³⁶ A. C. Potter and P. A. Lee, Phys. Rev. Lett. **105**, 227003 (2010).
- ³⁷ A. C. Potter and P. A. Lee, Phys. Rev. B **83**, 094525 (2011).
- ³⁸ Q.-F. Sun and X. C. Xie, J. Phys. Condens. Matter **21**, 344204 (2009).
- ³⁹ Q.-F. Sun, J. Wang, and T.-H. Lin, Phys. Rev. B **59**, 3831 (1999).